1. DEMONSTRATION OF A STATISTICAL, RULE-BASED FAULT DETECTION AND DIAGNOSTIC METHOD ON A ROOFTOP AIR CONDITIONING UNIT

Mark S. Breuker and James E. Braun, Ph.D.
Ray W. Herrick Laboratories, Purdue University
West Lafayette, IN 47907-1077, USA

This paper presents the results of the testing of a statistical, rule-based fault detection and diagnostic method on a rooftop air conditioning unit. When faults occur in the unit, the measured thermodynamic states differ from the states which are predicted by a model for normal system behavior, generating residuals. The magnitude and statistical uncertainty of the residuals determine the detection sensitivity of the technique. The directional changes in the residuals are statistically compared with a set of rules in order to diagnose a fault. By experimentally introducing faults to the air conditioning unit at five different operating conditions and recording the changes in output states, the detection sensitivity of the technique was quantified and the robustness of the diagnostic rules was verified. Results show that the technique is able to reliably detect refrigerant leakage, condenser fouling, evaporator fouling, liquid line restriction, and compressor valve leakage over a wide range of operating conditions, before a significant decrease in the capacity and COP has occurred. However, the sensitivity of the technique is influenced by the operating conditions of the unit.

2. Introduction

Fault detection and diagnostics (FDD) involves the application of artificial intelligence techniques to systems to monitor their health and to diagnose the cause of problems. Fault detection and fault diagnosis are the first two steps of process supervision described by Isermann (1984). Methods to perform FDD have been developed for a variety of complex systems, from the space shuttle main engine to nuclear power plants. As the costs of sensors and computer technology continue to fall, the ability to add FDD systems to equipment which is less critical and expensive than these examples continues to increase. In buildings, there is a growing interest in incorporating FDD techniques within energy management and control systems (Norford et al. 1987, Pape et al. 1991). In addition to applying FDD to large systems, there is also an opportunity to apply the technology to the subsystems in a building. FDD systems can increase efficiency and reliability and decrease service costs for vapor compression equipment by detecting faults which lead to a reduction in equipment efficiency and equipment life. Service costs can be decreased by using FDD systems to determine when service is justified, rather than doing regularly scheduled service or waiting for the equipment to break (Rossi & Braun, 1996). Some of the methods that have been developed to perform FDD on vapor compression equipment include work by Grimmelius et al. (1995), Stylianou & Nikanpour (1996), and Rossi & Braun (1997).

1.1 Motivation

Rooftop air conditioning systems are a good application for FDD for several reasons. First of all, the unit is an integrated system, allowing the sensors to be centralized in one location and to be factory installed. Secondly, rooftop units are often used in situations where there are no qualified personnel on staff to operate and maintain the equipment. Additional information could be provided to untrained building personnel by an FDD system to determine when service is required on the equipment, before a fault becomes so severe that the unit is unable to maintain comfort. A large service organization which has a contract to operate and maintain buildings might tie the FDD system to a remote communication unit which could report on the health of the equipment at regular intervals. This information would facilitate better work planning and an overall reduction in the cost to maintain building comfort.

A statistical, rule-based technique to perform fault detection and diagnostics on vapor compression air conditioners has been developed by Rossi and Braun (1997). The technique detects and diagnoses five distinct faults common to vapor compression equipment: 1) condenser fouling, 2) evaporator fouling, 3) refrigerant leakage, 4) liquid line restriction, and 5) compressor valve leakage. These faults will usually occur slowly over time and often go unnoticed until the equipment is unable to maintain comfort or they cause a more serious and expensive problem, such as a compressor failure. The technique uses a model to predict the expected values for temperatures in a normally operating unit as a function of the driving conditions. The expected temperatures are compared with current operating temperatures to generate residuals. The magnitudes of the residuals are statistically evaluated to perform fault detection and compared with a set of rules based on directional changes to perform fault diagnosis.

The method was developed using a detailed computer simulation model (Rossi, 1995) which solves the mass, energy, and momentum balances for vapor compression equipment given any set of driving conditions and fault levels. The model was used to determine which measurements are the most important for detection and diagnosis, to develop diagnostic rules, and to study the sensitivity of the technique to each fault for a given level of measurement error. The results of the sensitivity study did not consider the additional error introduced to the technique by imperfect model predictions. Some experimental verification of the technique was performed, but only at a limited range of operating conditions. The effect of compressor valve leakage was not verified experimentally.

1.2 Objectives

The overall goal of the research described in this paper was to provide further experimental evaluation of the FDD technique of Rossi and Braun (1997). The specific objectives of this research were:

- To provide a realistic estimate of the technique's sensitivity in detecting faults by accounting for error in the steady-state model prediction.
- To determine the effect of operating conditions on the diagnostic rules used by the FDD technique.

- To determine the effect of operating conditions on the detection sensitivity of the technique.
- To quantify, at the level at which faults can be detected, the change in the system's capacity and COP.

3. FDD Technique

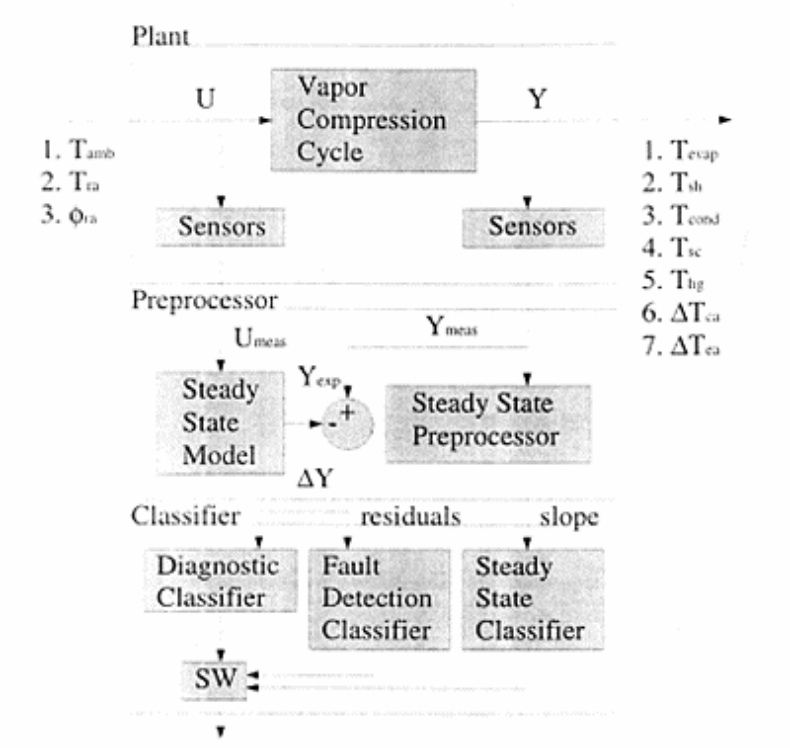

Figure 1: Structure of Fault Detection and Diagnostic Technique

The structure of the FDD technique is depicted in the block diagram of Figure 1. The technique requires the measurement of nine temperatures and one relative humidity on the rooftop unit. Three measurements, the temperature of the ambient air into the condenser coil (T_{amb}), the temperature of the return air into evaporator coil (T_{ra}), and the relative humidity of the return air into the evaporator coil (Φ_{ra}), are used to characterize the driving conditions (**U**) of the unit. In a normally operating, simple rooftop air conditioning unit (on/off compressor control, fixed speed fans), all the output states (**Y**) in the system are assumed to be functions of only these three driving conditions. The output state measurements used by this technique are five refrigerant temperatures and two air temperatures. They include: 1) evaporating temperature (T_{evap}), 2) suction line superheat (T_{sh}), 3) condensing temperature (T_{cond}), 4) liquid line subcooling (T_{sc}), 5) hot gas line or compressor outlet temperature (T_{hg}), 6) air temperature rise across the

condenser (ΔT_{ca}), and 7) air temperature drop across the evaporator (ΔT_{ea}). A steady-state model is used to describe the relationship between the driving conditions and the expected output states in a normally operating system. By comparing the measurements of the output states ($\mathbf{Y_{meas}}$) with those predicted by the steady-state model ($\mathbf{Y_{exp}}$), residuals ($\mathbf{\Delta Y}$) are generated. These residuals are used to perform detection and diagnosis. The detection classifier uses the residuals to determine a binary "fault" or "no-fault" output. The diagnostic classifier also uses the residuals to identify the most likely cause of the faulty behavior.

Since a steady-state model is used to predict normal operating states, a steady-state detector must be used to distinguish between transient and steady-state operation. Because a simple rooftop unit of this type would likely utilize "on/off" control, it will spend a significant amount of time in a transient condition. Glass et al. (1995) have suggested several methods which could be used to determine when the system is operating in a steady-state condition. The steady-state classifier provides a binary output to a switch (SW), which ignores the output of the detection and diagnostic classifiers unless the system is in steady-state.

1.3 Detection Classifier

The detection classifier uses residuals to determine whether the current equipment behavior is normal or faulty. The residuals are calculated by comparing the current output measurements with the expected output values generated by a steady-state model. When the current residuals are statistically different than the expected residuals (zero mean), a fault is identified.

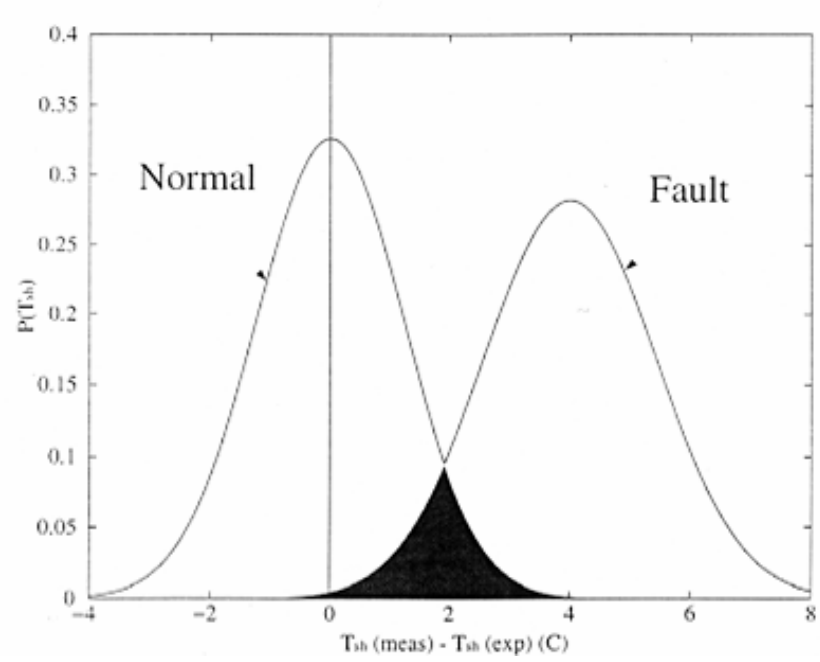

Figure 2: One Dimensional Example of Detection Classifier

In Figure 2, the two curves represent the probabilities [$P(T_{sh})$] of obtaining specific residuals for normal and faulty measurements. The uncertainty of the residuals is assumed to follow a Gaussian distribution. The integrated overlap of the two distributions, which indicates the likelihood that the faulty distribution of residuals represents normal operation, is termed the classification error. A fault in the system will cause a difference in the mean values and/or standard deviations of the residuals. As the fault becomes progressively worse, the difference between the mean values increases and the classification error decreases. Once the classification error drops below a threshold value, a fault is indicated by the detection classifier. In order to compare the current behavior with expected behavior using all seven output state measurements, an optimal linear classifier (Fukunaga 1990) is used. The residuals for the current and expected operation are fitted to a Gaussian model which can be completely described by the mean vector and covariance matrix (Rossi and Braun, 1997). A value of 10^{-3} is used as the threshold classification error in this paper.

1.4 Diagnostic Classifier

The role of the diagnostic classifier in the FDD system is to determine the most likely explanation of the faulty behavior occurring in the system. It compares the direction in which the output measurements change when a fault is introduced to the system with a set of rules. Table 1 shows the rules used for diagnosis. These rules were developed using a simulation model and tested experimentally at one operating condition.

Table 1: Rules for Diagnostic Classifier

Fault	T_{evap}	T_{sh}	T_{cond}	T_{sc}	T_{hg}	ΔT_{ca}	ΔT_{ea}
Refrigerant Leak	↓	↑	↓	↓	↑	↓	↓
Comp. Valve Leak	↑	↓	↓	↓	↓	↓	↓
Liquid Restriction	↓	↑	↓	↑	↑	↓	↓
Condenser Fouling	↑	↓	↑	↓	↑	↑	↓
Evaporator Fouling	↓	↓	↓	↓	↓	↓	↑

Each fault has a unique set of rules when compared using all seven measurements. By integrating the overlap of the current distribution with each of the fault classes described by the set of rules, the probability that the current behavior can be explained by each of the fault classes can be calculated and compared (Rossi and Braun 1997). The fault probability ratio is defined as the probability of the most likely fault to the second most likely fault. A fault probability ratio of 2 was used in this study as the threshold below which the output of the diagnostic classifier was considered invalid.

4. Experimental Set-up

1.5 System Description

The unit which was tested in this investigation is a three ton (10.55 kW) packaged rooftop air conditioning unit (Carrier Model 48DJE00416). It has constant speed motors

on both the compressor and the fans and capacity is controlled by cycling the compressor on and off. The expansion device is a fixed orifice type.

The indoor temperature and humidity and outdoor temperature were controlled using two psychrometric chambers. The rooftop unit is located in the chamber at outdoor conditions and air from the indoor chamber is brought to the rooftop unit through an insulated duct. A direct expansion vapor compression system is used to cool and dehumidify the air in the chambers. Control of the air temperature and relative humidity is achieved with electric heat and steam injection.

1.6 Measurements

Temperature measurements which were used for this analysis were taken using two types of sensors. The refrigerant temperatures were measured using K-type thermocouples which were soldered to the pipe surface and insulated. Surface temperatures are close to the refrigerant temperature and are sufficiently accurate for the FDD technique evaluated in this paper. RTD's were used to measure air temperatures. The specified measurement noise of the thermocouples and RTD's is less than +/- 0.5 C. The evaporator inlet and outlet relative humidities were measured using a capacitive polymer sensor with a published accuracy of +/-3% relative humidity in the range of conditions considered in these tests.

Pressure, flow, and power measurements were taken during this study to quantify the effect of the faults on the system. Pressures in the system were measured using pressure transducers with an accuracy of +/- 6.9 kPa (low side pressures) and +/-17.9 kPa (high side pressures). Flow measurements were taken using a Micromotion 25S-SS mass flow meter with an accuracy of +/- 0.4% of full scale. The mass flow meter, however, loses some accuracy if it operates over a wide range of pressures or if a two-phase mixture is present. These effects lead to a decrease in the accuracy of the meter in these tests. Power was measured using an AC watt transducer with an accuracy of +/- 32 W.

All measurements were processed using a Hewlett Packard HPE1326B multi-meter, and interpreted and recorded with a PC running the HPVee data acquisition software.

1.7 Fault Simulation and Characterization

All five faults were introduced experimentally to the rooftop unit via reproducible, quantifiable means. The methods used to introduce these faults are explained in this section.

Condenser fouling occurs in the field as a build-up of debris on the condenser coil. This build-up will cause a net loss of condenser surface area available to transfer heat from the refrigerant to the air. In the laboratory tests, condenser fouling was introduced by blocking the condenser coil with uniformly spaced, vertical paper strips. The level of fouling is expressed as a total % reduction in the surface area of the condenser coil. It was introduced at the following levels: 7.5%,15%, 22.5%,30% and 35% reduction in total condenser surface area.

Evaporator fouling is generally the result of a plugged air filter or a blocked return air vent. Unlike condenser fouling, it does not make sense to quantify this fault as reduction

in the area of the coil. Instead, this fault was simulated by partially blocking the air flow upstream of the evaporator coil. By measuring the change in differential pressure across the evaporator fan as a result of the blockage, a reduction in air flow rate was calculated from the fan curve. Air flow across the evaporator coil was reduced in approximately 10% increments.

A **liquid line restriction** can be caused by a plugged filter/dryer or some debris lodged in the fixed orifice expansion device. In either case, it results in an increased pressure drop in the liquid line. It was simulated in the experiments by partially closing a globe valve placed in the liquid line. The level of fault is characterized by the following ratio:

$$\text{Restriction Level} = 100\% * \frac{\Delta P_{res}}{\Delta P_{sys}} \quad (1)$$

where ΔP_{res} is the pressure drop across the restriction valve and ΔP_{sys} is the difference between high side (condensing) and low side (evaporating) pressures in the system before a restriction fault is introduced. The restriction valve was closed to achieve restriction levels of approximately 2.5% increments.

A **compressor valve leakage** is one cause of a reduction in the capacity of a compressor. It is typically caused by slugs of liquid refrigerant which damage the suction valve in the compressor, causing it to lose an effective seal. When this happens, some of the high pressure refrigerant in the compression cylinder leaks back into the suction line across the suction valve. This results in a reduction in the volumetric efficiency of the compressor. A compressor valve leakage was simulated by opening a globe valve which allows gas from the discharge line to recycle into the suction line. The % reduction in the net volumetric efficiency of the compressor is calculated using the known compressor specification, the inlet refrigerant state, and the mass flow measurement. The net volumetric efficiency of the compressor was reduced in approximately 2% increments.

Refrigerant leakage is simply the loss of refrigerant from the system. It was simulated by discharging a fixed amount of refrigerant from the rooftop unit into a receiving vessel and weighing the vessel before and after the discharge. The level of refrigerant leakage is quantified as the % reduction in the total charge in the system. Refrigerant was removed from the system in approximately 2.5% increments.

5. FDD Evaluation Approach

1.8 Characterization of Measurement and Modeling Errors

The uncertainties in the measurements and modeling predictions have a large effect on the sensitivity of the technique in detecting faults in the system. In the one-dimensional example shown in Figure 2, the amount of uncertainty in the measurements and the model predictions will increase the standard deviation of both the expected (normal) and current (faulty) distributions of residuals, causing them to become wider. As the uncertainty increases, the difference between the mean vectors, and, therefore, the level of fault, must be greater before the integrated overlap of the two distributions (classification error) is less than the threshold value. This reduces the sensitivity of the FDD technique. When considering all seven measurements in the detection and

diagnostic classifiers, the overall uncertainty in the residuals due to measurement and modeling errors are represented by the covariance matrix. The effect of measurement and modeling error on the covariance matrix is considered in this section.

Measurement noise will increase the uncertainly of the distribution of residuals in two ways. Consider the measurements shown in Figure 1. First, the sensor noise will introduce error in the direct measurement of the output states ($\mathbf{Y_{meas}}$). In addition, the error in the measurement of the input states **($\mathbf{U_{meas}}$)** of the model will propagate through the model, causing error in the prediction of the output states **($\mathbf{Y_{exp}}$)**. These two effects were included in the previous sensitivity results given by Rossi and Braun (1997).

In addition to measurement error, a model will be unable to give a perfect prediction for the system output states, even if it is given perfect measurements for the input states. Error in the steady-state model predictions will result from: 1) driving conditions which are not accounted for in the model, and 2) an imperfect model form to map the relationship between inputs and outputs.

It is inevitable that driving conditions which cannot be easily quantified or are unexpected will have an effect the system performance. An example of a driving condition which is unaccounted for in this model is solar radiant energy on the condenser coil. Although the amount of radiant energy gained by the coil is expected to be small when compared with the energy lost from the coil due to convection, it may cause the unit to operate slightly differently at the same apparent driving conditions.

Even when all of the important inputs are considered, a steady-state model with a finite number modeling coefficients can not perfectly describe the relationship between the inputs and outputs given in the training data. In this case, the modeling error depends on the extent of the nonlinear relationship between inputs and outputs, the model form which is chosen, and the method used in learning the model.

To account for the effect of measurement and modeling errors, Equations (2) and (3) were used to construct the diagonal and off-diagonal elements in the i^{th} row and j^{th} column of the covariance matrix used to characterize the distributions of residuals.

$$\Sigma_{ij} \approx \sigma_T^2 + \sigma_{M,i}^2 + \left(\frac{\partial f_i}{\partial \mathrm{T_{amb}}}\right)^2 \sigma_T^2 + \left(\frac{\partial f_i}{\partial \mathrm{T_{ra}}}\right)^2 \sigma_T^2 + \left(\frac{\partial f_i}{\partial \Phi_{\mathrm{ra}}}\right)^2 \sigma_\Phi^2 \text{ , i = j} \qquad (2)$$

$$\Sigma_{ij} \approx \left(\frac{\partial f_i}{\partial \mathrm{T_{amb}}}\right)\left(\frac{\partial f_j}{\partial \mathrm{T_{amb}}}\right)\sigma_T^2 + \left(\frac{\partial f_i}{\partial \mathrm{T_{ra}}}\right)\left(\frac{\partial f_j}{\partial \mathrm{T_{ra}}}\right)\sigma_T^2 + \left(\frac{\partial f_i}{\partial \Phi_{\mathrm{ra}}}\right)\left(\frac{\partial f_j}{\partial \Phi_{\mathrm{ra}}}\right)\sigma_\Phi^2, \text{ i} \neq \text{j} \qquad (3)$$

where:

Σ_{ij} is the element in the i^{th} row and j^{th} column of the covariance matrix.

f_i is the steady-state model prediction for output *i*.

σ_T^2 = $E(w_T^2)$, where w_T is zero mean noise added to the temperature measurements (measurement error) and E( ) is the expected value operator.

$\sigma^2_{M,i}$ = $E(w_{M,i}^2)$, where $w_{M,i}$ is zero mean noise added to the model predictions (modeling error) for output *i*. E( ) is the expected value operator.

σ^2_{Φ} = $E(w_{\Phi}^2)$, where w_{Φ} is zero mean noise added to the relative humidity measurements and E( ) is the expected value operator.

This analysis assumes that the steady-state model output can be expressed as an predicted value (f_i) plus a zero mean, normally distributed error term ($\sigma_{M,i}^2$) . This analysis also assumes that the steady-state model can be approximated by a Taylor series approximation about the known operating point (Rossi & Braun 1997). To quantify the error in the model outputs due to input measurement error, the partial derivatives of the model outputs with respect to each of the inputs must be known. These partial derivatives were evaluated numerically using a simple steady-state model which was developed for the rooftop unit from experimental data. This model uses data for the output measurements which were recorded over a 5x5x5 grid of driving conditions (T_{amb}, T_{ra}, and Φ_{ra}). This data was placed in a regularly spaced lookup table. A series of 1 dimensional linear interpolations were used to calculate the outputs for driving conditions which did not lie exactly on the grid points in the table.

1.9 Approximations for Measurement and Modeling Error

In this study, conservative estimates for sensor error were used. For temperature measurements, a 0.5 C standard deviation of error was used. For the relative humidity, the standard deviation of error was assumed to be 5%.

There is be a different amount of modeling error associated with each of the seven output measurements used in the FDD method. Based upon initial modeling of laboratory test results for normal operation, a standard error of 0.3 C was assumed for all the measurements except suction superheat and hot gas temperature. T_{sh} and T_{hg} appear to be more difficult to predict than the rest and are characterized with a higher standard deviation of error (1.0 C).

Figure 3 shows the trend of suction superheat to "accelerate" toward zero at high ambient temperatures. When the superheat is small (< 5 C), small changes in the operating conditions can cause large changes in superheat. This non-linear change in the behavior for suction superheat has a cascading effect on the hot gas temperature. This non-linear relationship is difficult to characterize with a model.

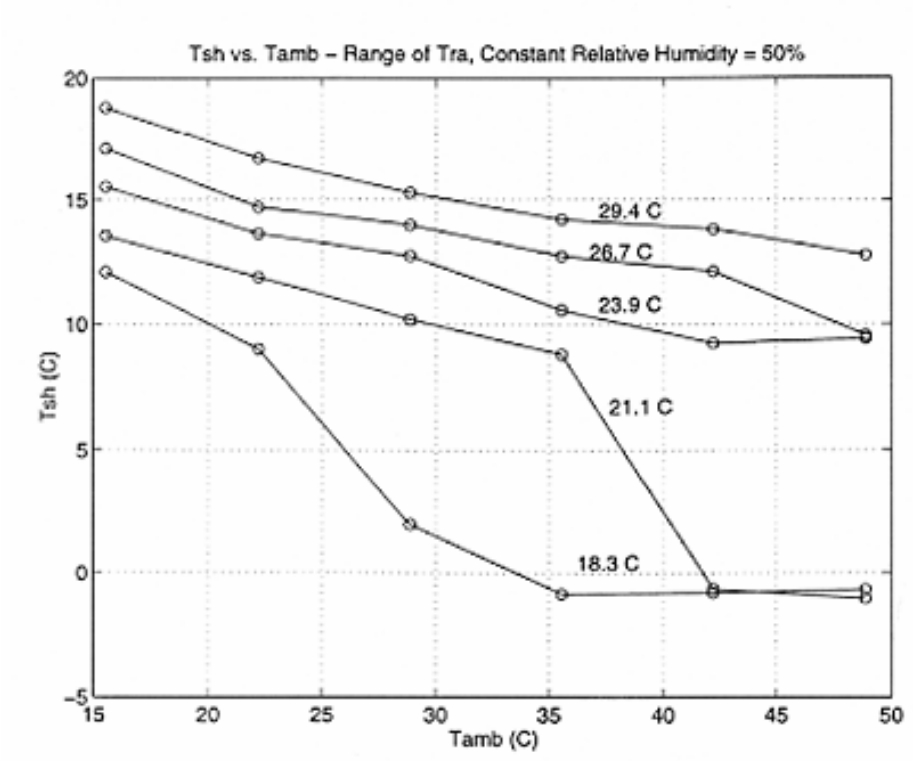

Figure 3: Suction superheat vs. T_{amb} - Lines of constant T_{ra}

1.10 Summary of Testing Procedures

Each of five faults were introduced at five separate operating conditions. The five conditions which were tested are listed in Table 2. These conditions represent a base point and four extreme types of operation.

Table 2: Operating Conditions Tested

Condition	T_{amb} (C)	T_{ra} (C)	Φ_{ra}
Normal	28.9	21.1	50%
Low Load	18.3	19.4	40%
High Load	44.4	27.8	55%
Low T_{sh}	37.8	20.0	40%
High T_{sh}	18.3	25.6	60%

Normal operation at each set of driving conditions was first recorded with no faults present. The faults were then each introduced at a minimum of 4 distinct levels while keeping the driving conditions constant. Measurements were taken every five seconds for all of the input and output variables. After the system came to steady state, the mean values for the output measurements were calculated by averaging the data in a window with a minimum of 20 steady-state measurements. The residuals were calculated by subtracting the output state measurements at each fault level from the output state measurements which were recorded for normal operation.

1.11 Estimating FDD Sensitivities

Once the elements of the covariance matrix have been calculated, the sensitivity of the technique to different faults will depend on the relationship between the fault level and the size of the residuals. It is expected that as the fault level is increased, the magnitudes of the residuals will increase. If the magnitudes of the residuals increase in the expected directions, the detection error decreases and the fault probability ratio increases. The sensitivity of the technique to each fault is defined as the level of fault which needed to be introduced to the system for it to be successfully detected and diagnosed. A fault was detected and diagnosed once the classification error dropped below 10^{-3} and the fault probability ratio exceeded 2. Linear interpolation of the experimental results was used to approximate the residuals at fault levels which were between the fixed levels introduced during the experiments.

6. FDD System Test Results

1.12 Refrigerant Leakage

The rules used to diagnose a refrigerant leakage shown in Table 1 held in all of the tests which were conducted. The detectable level of the refrigerant leakage and its corresponding effect on system capacity and COP at all five test conditions are shown in Table 3.

Table 3: Detectable Level of Refrigerant Leakage

Quantity	Normal	High Load	Low Load	High T_{sh}	Low T_{sh}	Average
% Loss of Refrigerant	6.4	12.1	7.7	7.0	5.2	7.7
% Change in Capacity	-4.0	-17.3	-6.7	-8.8	-7.3	-8.8
% Change in COP	0.0	-7.5	-2.9	-4.7	-6.8	-4.4

The technique performed well at all conditions except the High Load case. In this case the fault was not detected and diagnosed until the system lost 12.1% of its refrigerant and 17.3% of its capacity. The reduction in FDD sensitivity for this case is best explained by comparing the results of Figure 4 and Figure 5. Figure 4 shows effect of a reduction in refrigerant charge on the classification error and fault probability ratio for the Low T_{sh} test. The **Threshold** line indicates a detection classification error of 10^{-3} on the left axis and a fault probability ratio of 2 on the right axis. A fault is detected and diagnosed once the **Error** drops below the **Threshold** and the **Ratio** exceeds the **Threshold**. In this case, the threshold for classification error is reached slightly after the fault probability ratio reaches its threshold. The fault is detected and diagnosed after 5.2% of the charge has leaked from the system.

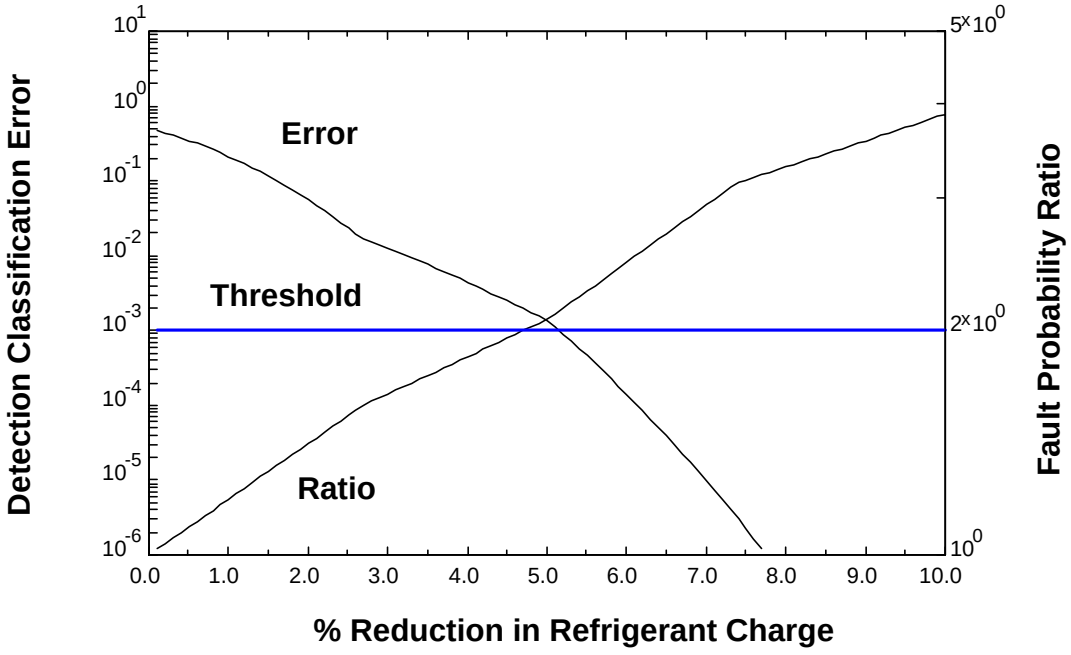

Figure 4: Refrigerant Leakage FDD Sensitivity: Low T_{sh} Conditions

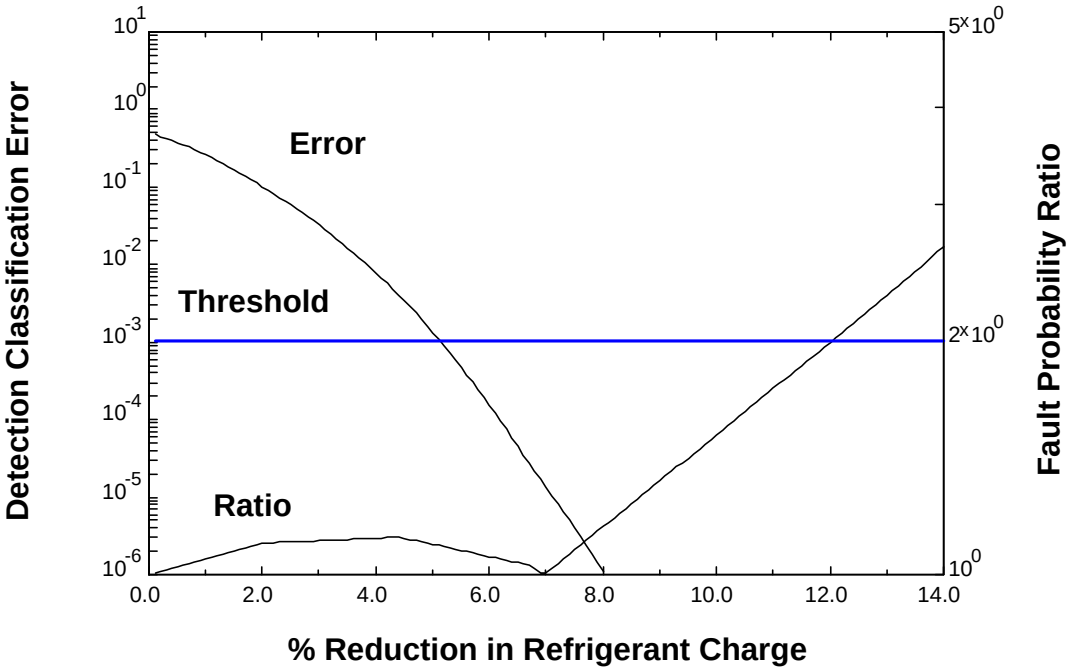

Figure 5: Refrigerant Leakage FDD Sensitivity: High Load Conditions

Figure 5 shows classification error and fault probability ratio results for the High Load test. In this case, the fault probability ratio does not reach its threshold until 12.1% of the refrigerant has been removed from the system. The classification error dropped below its threshold at a 5.2% charge reduction. However, the diagnostic classifier could not distinguish between a refrigerant leakage and a liquid line restriction until significantly more refrigerant was removed. Table 1 shows that the rules are the same for these two faults in all measurements except for liquid subcooling. At High Load conditions, the subcooling initially increased a small amount as refrigerant was removed, giving a weak indication of a liquid line restriction. Eventually, the subcooling started to decrease and the diagnostic classifier correctly identified the refrigerant leakage fault. A high ambient temperature causes a low level of subcooling and a loss of sensitivity of the subcooling residual to a refrigerant leakage. This theory is supported by the fact that the Low T_{sh} test, the other high ambient test, also showed a smaller than average change in subcooling.

The size of the residuals at the level at which refrigerant leakage was detected and diagnosed is shown in Figure 6. These results show that the suction superheat (T_{sh}), hot gas temperatures (T_{hg}), and the evaporating temperature (T_{evap}) are the most sensitive residuals for a refrigerant leakage.

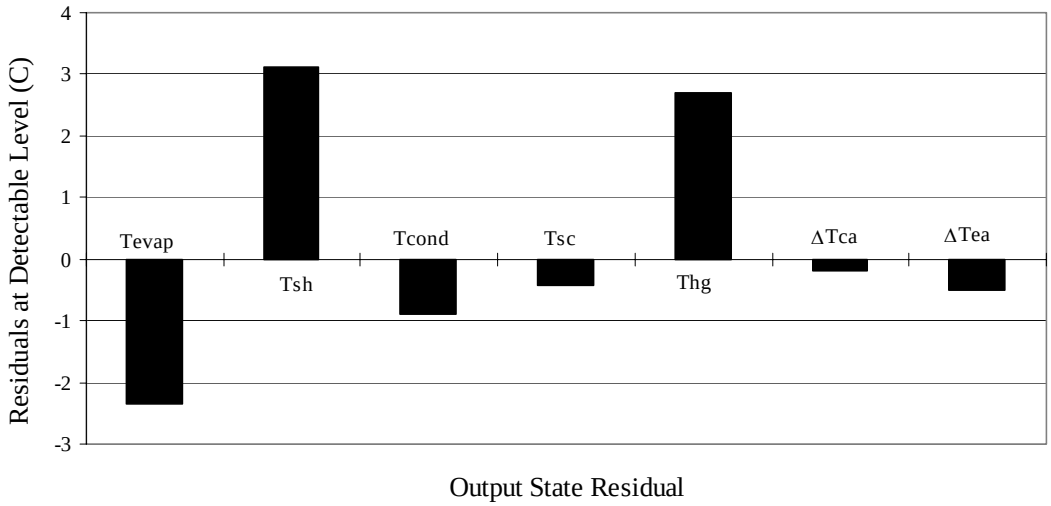

Figure 6: Average Residuals at Detectable Level of Refrigerant Leakage

1.13 Condenser Fouling

The rules used to diagnose condenser fouling shown in Table 1 also held at all five operating conditions. The detectable level of the condenser fouling fault and its corresponding effect on system capacity and COP at all five test conditions are shown in Table 4. Condenser fouling was detected at all five test conditions before a 6% decrease in capacity occurs. The FDD sensitivity to condenser fouling decreases slightly at high ambient conditions, but is relatively insensitive to operating conditions. In Normal and High T_{sh} tests, a slight increase in capacity was calculated using a refrigerant side energy balance. This increase is most likely due to the difficulty in accurately measuring refrigerant mass flow rate coupled with the relatively small change in system performance at the detectable level of condenser fouling An actual increase in capacity due to condenser fouling does not make sense physically.

Table 4: Detectable Level of Condenser Fouling

Quantity	**Normal**	**High Load**	**Low Load**	**High T_{sh}**	**Low T_{sh}**	**Average**
% Decrease in Coil Area	28.5	28.5	28.1	23.8	31..8	28.1
% Change in Capacity	2.0	-1.7	-0.7	1.9	-5.5	-0.8
% Change in COP	-1.9	-6.0	-4.6	-3.1	-8.9	-4.9

The average residuals at the detectable level of condenser fouling are shown in Figure 7. As one might expect, the condensing temperature is the most sensitive residual for condenser fouling. For diagnosis, the temperature difference of the air across the condenser is an important measurement, since a condenser fouling fault is the only fault which causes this residual to increase.

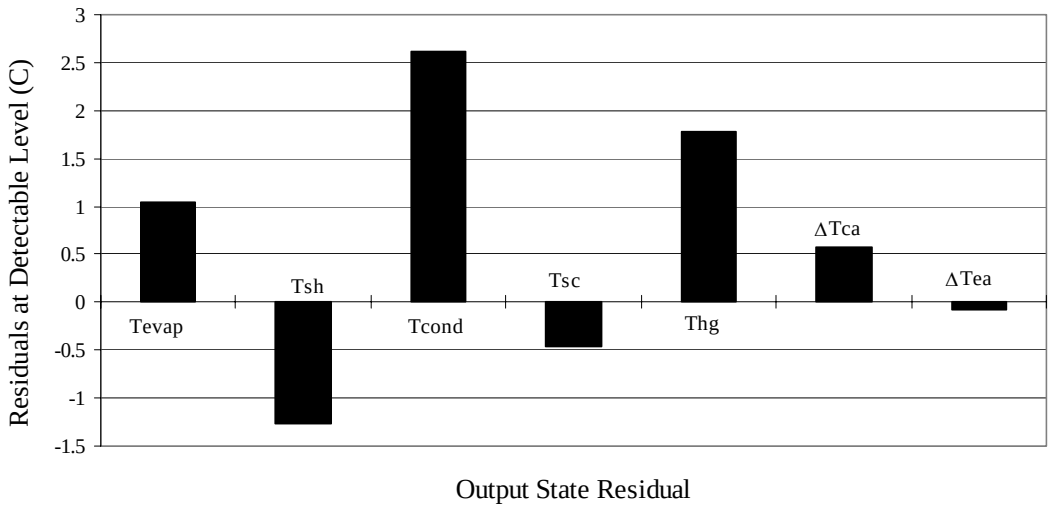

Figure 7: Average Residuals at Detectable Level of Condenser Fouling

1.14 Evaporator Fouling

The rules used to diagnose evaporator fouling shown in Table 1 also held at all five operating conditions. The detectable level of the evaporator fouling fault and its corresponding effect on system capacity and COP at four test conditions are shown in Table 5. The detection classifier was unable to detect evaporator fouling at the levels which were introduced at the High Load condition. The technique performed well at Normal, Low Load, and High T_{sh} conditions, detecting and diagnosing an evaporator fouling fault before the capacity or COP changed by more than 4%. The High Load and Low T_{sh} test, which both involve high ambient temperatures, were significantly less sensitive to the evaporator fouling.

Table 5: Detectable Level of Evaporator Fouling

Quantity	**Normal**	**High Load**	**Low Load**	**High T_{sh}**	**Low T_{sh}**	**Average**
% Decrease in Air Flow	34.1	> 42.5	17.9	21.0	21.1	23.5
% Change in Capacity	0.6	> 0.2	-3.5	-2.8	-12.1	-4.5
% Change in COP	3.7	>0.2	-0.9	-1.8	-9.1	-2.0

The average residuals generated at the detectable level of evaporator fouling are shown in Figure 8. The T_{sh} and the T_{hg} residuals are again the most sensitive to the fault. In terms of diagnostics, however, the temperature difference across the evaporator is the most important measurement, since evaporator fouling is the only one of the five faults which causes this temperature difference to increase.

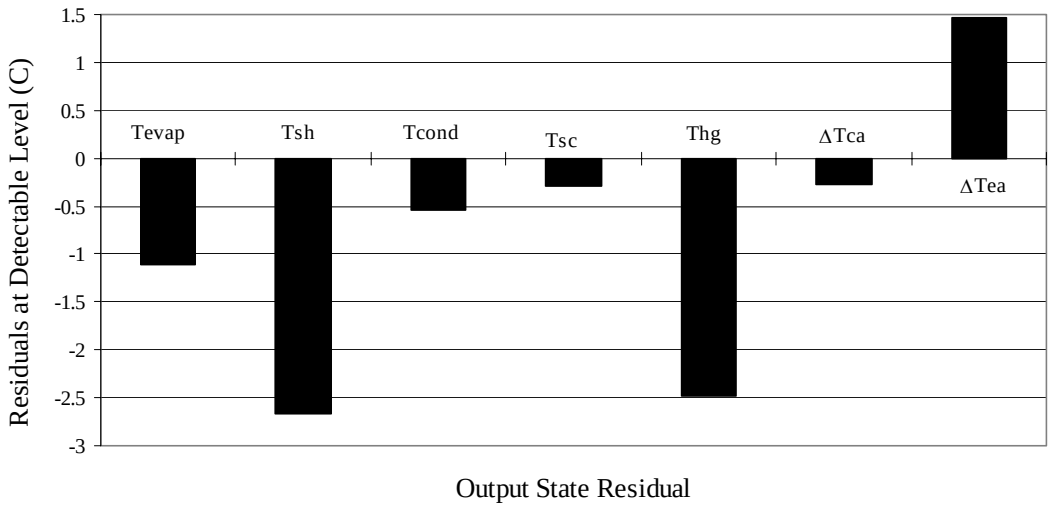

Figure 8: Average Residuals at Detectable Level of Evaporator Fouling

1.15 Liquid Line Restriction

The rules used to diagnose a liquid line restriction shown in Table 1 also held at all five of the operating conditions. The detectable level of the liquid line restriction fault and its corresponding effect on system capacity and COP at the five test conditions are shown in Table 5. In terms of restriction level, capacity, and COP, the technique is again the least sensitive at High Load conditions. In terms of the effect on capacity, the technique was significantly more sensitive at Normal and Low T_{sh} conditions.

Table 6: Detectable Level of Liquid Line Restriction

Quantity	Normal	High Load	Low Load	High T_{sh}	Low T_{sh}	Average
Restriction Level (Eq. 3)	11.2	16.1	9.2	7.2	9.0	10.5
% Change in Capacity	-2.9	-15.7	-6.7	-7.1	1.7	-6.1
% Change in COP	-0.5	-11.9	-3.8	-3.2	2.4	-3.4

The average residuals for a detectable level of liquid line restriction fault are shown in Figure 9. Again, T_{sh} and T_{hg} are the most sensitive of the measurements to the introduction of a fault.

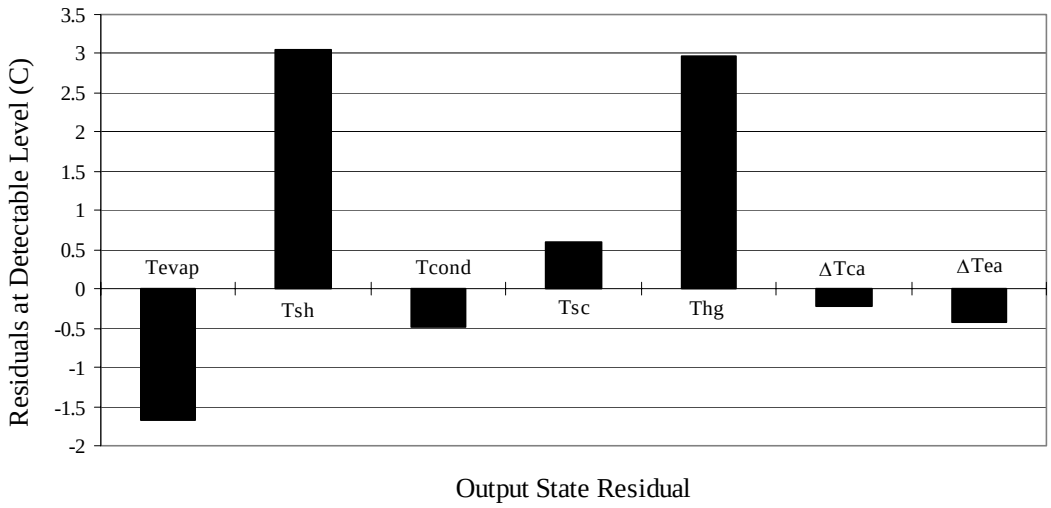

Figure 9: Average Residuals at Detectable Level of Liquid Line Restriction

1.16 Compressor Valve Leak

The rules for diagnosis of a compressor valve leakage, which were developed through simulation, did not hold during the experimental introduction of the fault. The rule which needed correction was the direction of the T_{hg} residual. Depending on the operating conditions, the hot gas temperature may either increase or decrease with compressor valve leakage. The hot, high pressure gas which recycles back into the suction line from the discharge line raises the temperature of the suction gas. At a constant pressure ratio, the recycled gas would cause the temperature of the compressor discharge gas to increase. However, a compressor valve leakage also causes a reduction in the pressure ratio, which will tend to decrease T_{hg}. Thus, the direction in which T_{hg} moves during a compressor valve leakage is a trade-off between these two effects. At Low Load and Normal conditions, the hot gas temperature decreased. At the other conditions, the hot gas temperature increased. This is the one rule which appears to change as a function of the operating conditions. The simulation model did not account for the effect of the hot, recycled gas on the suction line temperature since it modeled a compressor valve leak simply as a reduction in the compressor volumetric efficiency.

The rule for T_{hg} was updated to expect an increase in the hot gas temperature when a compressor valve leak is present. With the rule for T_{hg} updated, a sensitivity analysis for compressor valve leakage was performed. The detectable level of the compressor valve leakage fault and its corresponding effect on system capacity and COP at the five test conditions are shown in Table 7. The sensitivity to a compressor valve leak is comparable to the sensitivity to the other faults at all conditions except for the Low T_{sh} conditions. As with the other faults, the least sensitive cases for compressor valve leakage are the high ambient temperature tests. The Normal case, where the air conditioner will likely spend most of its operating time, is still quite sensitive to a compressor valve leak in terms of the effect on capacity.

Table 7: Detectable Level of Compressor Valve Leakage

Quantity	Normal	High Load	Low Load	High T_{sh}	Low T_{sh}	Average
% Decrease in Vol. Eff.	7.7	13.6	7.9	13.8	16.3	11.9
% Change in Capacity	-1.4	-6.9	-0.9	-5.5	-17.1	-6.4
% Change in COP	-3.3	-10.9	-1.7	-7.0	-21.0	-8.8

The average residuals generated at the detectable level of compressor valve leakage are shown in Figure 10. T_{sh} and T_{evap} are the most sensitive residuals to the introduction of a compressor valve leakage.

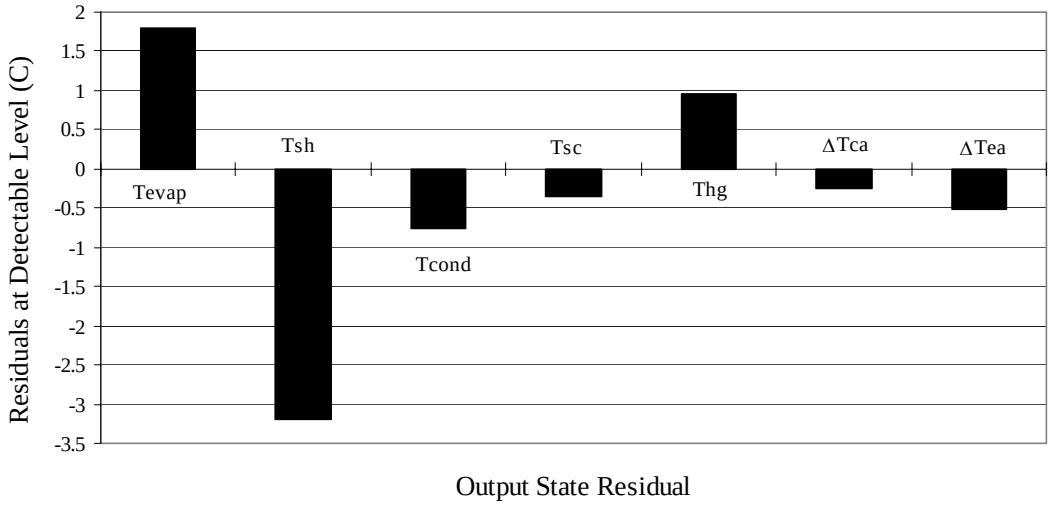

Figure 10: Average Residuals at Detectable Level of Compressor Valve Leakage

7. Conclusions/Future Work

This paper has reported on the testing of a statistical, rule-based fault detection and diagnostic technique on a simple rooftop air conditioning unit. The technique compares the current operating states with the expected states generated by a steady-state model to generate residuals. These residuals are statistically compared to the expected zero-mean distribution of residuals to detect a fault. They are compared to a set of rules based on the directional change of the residuals to perform diagnosis of the fault. The technique was experimentally tested at five different conditions to quantify the sensitivity of the technique over a range of driving conditions and to verify that the diagnostic rules did not break down. Noise was introduced into the expected and current distributions of residuals to account for measurement and modeling error.

A summary of the FDD sensitivity averaged over all five operating conditions which were tested is shown in Table 8. The results in Table 8 show that the technique was able to detect and diagnose these five commonly occurring faults in vapor compression equipment before they would have a significant impact on the operation of the equipment. The results also showed that the level at which the faults can be detected and diagnosed was dependent on the operating conditions. The technique was the least sensitive to faults when operating at high ambient conditions.

Table 8: Average Sensitivity of FDD Technique

Quantity	**Condenser Fouling**	**Evaporator Fouling** **(High Load Case Not Included)**	**Refrig. Leak**	**Liquid Line Restriction**	**Comp. Valve Leak**
Fault Level	28.1	23.5	7.7	10.5	11.9
% Capacity Change	-0.8	-4.5	-8.8	-6.1	-6.4
% COP Change	-4.9	-2.0	-4.4	-3.4	-8.8

Two problems with the diagnostic rules were identified which require further investigation. The dependency of refrigerant leakage diagnosis on the liquid line subcooling state was shown to be a problem at high ambient conditions, where the subcooling becomes less sensitive to a loss of refrigerant charge. Also, the rule for hot gas temperature used to diagnose a compressor valve leak was incorrect. The change in the hot gas temperature due to a compressor valve leak is dependent on the operating conditions.

The suction superheat and hot gas temperature residuals which were the most sensitive to the five faults. However, they are also the most difficult states to predict with a steady-state model.

Additional work to further demonstrate this technique should be directed toward the development and testing of a steady-state model and steady-state detector. This study assumed model predictions with a normally distributed error term. In practice, a real model will give a biased prediction of the expected output states at different operating conditions. Techniques to efficiently and accurately learn a steady-state state model should also be investigated. Once a steady-state model and detector have been developed, then on-line testing of the technique can take place.

8. Nomenclature

E( ) expected value operator
f_i plant model for i_{th} output
P( ) probability density function
T_{amb} ambient temperature (inlet to condenser)
T_{cond} condensing temperature
T_{evap} evaporating temperature
T_{hg} hot gas temperature (compressor outlet)

T_{ra} return air temperature (inlet to evaporator)
T_{sc} liquid line subcooling
T_{sh} suction line superheat
U vector of inputs that affect plant performance, driving conditions
Y vector of measured plant outputs
ΔP_{res} pressure difference across liquid line restriction valve
ΔP_{sys} difference between high side and low side system pressures for normal operation
ΔT_{ca} air temperature rise across condenser
ΔT_{ea} air temperature drop across evaporator
ΔY vector of residuals between measured and modeled plant outputs
Φ_{ra} return air relative humidity (inlet to evaporator)
σ standard deviation of measurements or modeling error
Σ covariance matrix for residuals

Subscripts
exp model prediction (expected performance predictions)
meas measured
T temperature
M model
Φ relative humidity

9. References

Fukunaga, K. 1990. *Introduction to Statistical Pattern Recognition.* W. Lafayette, IN: Academic Press.

Glass, A.S., P. Gruber, M. Roos, & J. Tödtli. 1995. Qualitative Model-Based Fault Detection in Air-Handling Units. *IEEE Control Systems Magazine* 15(4):11-22.

Grimmelius, H.T., J. Klein Woud, and G. Been. 1995. On-Line Failure Diagnosis for Compression Refrigeration Plants. *International Journal of Refrigeration* 18(1): 31-41.

Isermann, R. 1984. Process Fault Detection Based on Modeling and Estimation—A Survey. *Automatica* 20(4): 387-404.

Norford, L.K., A. Rabl, & G.V. Spadaro. 1987. Energy Management Systems as Diagnostic Tools for Building Managers and Energy Auditors. *ASHRAE Transactions* 93(2): 2360-2375.

Pape, F.L.F., Mitchell, J.W., & Beckman, W.A. 1991. Optimal Control and Fault Detection in Heating, Ventilating, and Air-Conditioning Systems. *ASHRAE Transactions: Symposia, Part 1* pp. 729-736. NY-91-10-05.

Rossi, T.M. 1995. Detection, Diagnosis, and Evaluation of Faults in Vapor Compression Cycle Equipment, Ph.D. Thesis, School of Mechanical Engineering, Purdue University.

Rossi, T.M. & J.E. Braun. 1996. Minimizing Operating Costs of Vapor Compression Equipment with Optimal Service Scheduling, *International Journal of Heating, Ventilating, and Air Conditioning and Refrigerating Research* 2(1): 23-47.

Rossi, T.M. & J.E. Braun. 1997. A Statistical, Rule-Based Fault Detection and Diagnostic Method for Vapor Compression Air Conditioners, *International Journal of Heating, Ventilating, and Air Conditioning and Refrigerating Research* 3(1): 19-37.

Stylianou, M. & D. Nikanpour. 1996. Performance Monitoring, Fault Detection, and Diagnosis of Reciprocating Chillers. *ASHRAE Transactions* 102(1): 615-627.